FASTC-ID(RS)T-0853-92

FOREIGN AEROSPACE SCIENCE AND TECHNOLOGY CENTER

NEW ALGORITHM OF GROUND TRACK PROCESSING IN HIGH-FREQUENCY SKYWAVE OVER-THE-HORIZON-B RADAR

by

Jiao Peinan

DISCLAIMER NOTICE

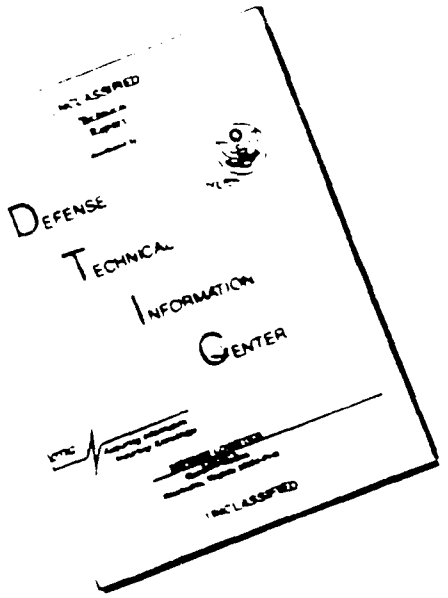

THIS DOCUMENT IS BEST QUALITY AVAILABLE. THE COPY FURNISHED TO DTIC CONTAINED A SIGNIFICANT NUMBER OF PAGES WHICH DO NOT REPRODUCE LEGIBLY.

HUMAN TRANSLATION

FASTC-ID(RS)T-0853-92 6 August 1993

MICROFICHE NR: 93C000497

NEW ALGORITHM OF GROUND TRACK PROCESSING IN HIGH-FREQUENCY SKYWAVE OVER-THE-HORIZON-B RADAR

By: Jiao Peinan

English pages: 15

Source: Dianzi Xuebao, Vol. 19, Nr. 1, 1991; pp. 1-6

Country of origin: China
Translated by: Leo Kanner Associates
F33657-88-D-2188
Requester: FASTC/TAER/Lt Thomas E. Deeter

PREPARED BY:

TRANSLATION DIVISION
FOREIGN AEROSPACE SCIENCE AND TECHNOLOGY CENTER
WPAFB, OHIO

GRAPHICS DISCLAIMER

All figures, graphics, tables, equations, etc. merged into this translation were extracted from the best quality copy available.

NEW ALGORITHM OF GROUND TRACK PROCESSING IN HIGH-FREQUENCY SKYWAVE OVER-THE-HORIZON-B RADAR

Jiao Peinan

China Research Institute of Radio Wave Propagation, Xinxiang

Abstract: In the paper, the concept pattern of the recognition-tracking-coordinate transformation data processor in HF skywave OTH-B radar is described. A new algorithm to determine the ground distance of a moving object from the time delay transformation of HF radar is proposed. Just the probe data obtained from only a single radar station are needed; there is no need to know the midpoint ionospheric data. The calculated ground track is compared with the actual track and the results show that the mean deviation is less than 4 percent.

I. Introduction

The shortwave skywave reentry scattering over-the-horizon radar (briefly referred to OTH-B radar in the following) serves in utilizing the skywave reentry scattering propagation regime from the ionosphere in order to probe a long-range target over the horizon; this is a new radar system [1]. This is a relatively promising and more economical means of advance warning of penetration by low-flying aircraft. This also has great potential in monitoring ships on the high seas and marine meteorology.

Since the OTH-B radar operates in the shortwave band, and the ionosphere with random time-varying color dispersion is used as the propagation medium, in addition, the direction graph of the vertical plane of the antenna array shows the wideband beam, therefore this method of radar ground track processing is much different and more difficult than the visual-distance microwave radar.

As recorded by OTH-B radar, the parameters of point tracks of the target are: target radar time delay P, doppler frequency f_d, target orientation θ, working frequency f, and probe time t. Data processing involves the following features: (1) the complex multilayer configuration and propagation route in the ionosphere generate the mode fuzziness and multipath effect of point tracks; it is required to conduct pattern recognition on the propagation of point tracks. (2) The time delay P of radar should be converted into great-circle path D of geographical coordinates in order to be the final output to the command center. This transformation is related to the real-time states of working frequency and ionosphere. (3) Because of serious shortwave environmental noise and interference, the existence of false targets in nature, movement of the ionosphere, and radar target dimensions are in the resonance zone, causing echo attenuation, relatively high false alarms and false dismissal probabilities exist for the point tracks, causing discontinuity of the point tracks. (4) The time intervals between track sampling is of the order 10s, therefore the tracking algorithm should not use the α-β filtration criterion commonly employed by visual-distance radar; instead, the Karman filtration criterion should be adopted.

The final determination of completing a ground track by OTH-B radar generally takes 10-20min. However, for OTH-B radar with operating distance of 3000km an aircraft can cover only

300km in 20min even at a speed as high as 1000km/h. There is still sufficient time to organize interception.

The paper briefly describes the key techniques of a ground track processor in OTH-B radar, that is, the concept of pattern recognition, tracking, and data processing of coordinate transformation. This algorithm emphasizes the study of transforming the radar time delay P into the ground distance D as closely related to real-time ionospheric states. In the new algorithm described here, it is not necessary to assume or adopt data other than the radar station as in previous methods; the algorithm can be executed by using just the probe data of equipment at a single radar station. The following are the features: sparse data to be processed, high property in real-time status, and algorithmic simplicity. Using this method to process experimental data in OTH-B radar, the resulting ground tracks match with the ground tracks given by a navigation guidance station. The mean deviation is less than 4 percent.

II. Concept of Pattern Recognition Tracking Device

By using pattern recognition, tracking and data processing of coordinate transformation, the ground track processor differs widely from the ground track processor of microwave visual-distance radar.

1. Pattern fuzziness multipath effect

Due to the complex multilayer configuration of the ionosphere, the path of radar beams is often a combination of propagation paths of these different layers, thus forming multimode propagation. Even if there were only a single layer, due to the existence of high and low beams, there may also be possibly formed three propagation modes, including blended modes. However, appropriate selection of operating parameters such as

working frequency can achieve the purpose of reducing the number of modes. However, in the process of probing and tracking a moving target by a radar, the chance of an exclusively single-mode propagation is low.

Multimode propagation leads to two different results when radar probes a target: one is the mode fuzziness effect and the other is the multipath effect. In the former case, multiple targets may possibly considered a single target. In the latter case, a single target may be possibly determined to be multiple targets.

From the principle, if the OTH-B radar has an antenna array with very narrow vertical plane wavebeam to probe the arrival angle of incoming wave, then the radar can determine the propagation mode within a single dwell time. Due to considerations of economy and technique, OTH-B radar generally employs an antenna array of narrow horizontal plane, but wide vertical plane in the wavebeam, thus special techniques are required to determine the propagation mode for the radar.

2. Pattern recognition of propagation mode

In the OTH-B radar system, the subsystem of ionosphere reentry scattering probe and the main radar share the same radar antenna array. By continuous frequency-shift probing in the radar probe direction, the boundary of the $P \sim f$ relationship corresponding to all the frequencies (3 to 30MHz) and all the radar echo time delays (500 to 3200km) is called the observable-zone mode. These radar echoes are the result of the ground scattering energy and the near-ground target scattering energy propagated via a particular mode.

Fig. 1 is a schematic diagram for the mode of the $P \sim f$ ionization diagram simplified by an ionosphere with a two-layer

configuration. The diagram indicates an observation zone of two modes for the F- and E-layers; the overlapping part is called the mode fuzziness zone of F-E layer. Obviously, if the frequency is f_1 and the target point tracks are di covered in the not-fuzziness mode, the mode can be determined uniquely. If the target point tracks are discovered in the fuzziness-zone mode, it is not possible to uniquely determine which propagation mode is involved. To understand mode fuzziness, another observation is needed by jump-shifting the working frequency so that the point tracks are away from the fuzziness zone or intersect with its boundary. If the frequency jumps to f_2 and the point tracks fall on the boundary of zone F, and then the frequency jumps to f_3, and does not appear in zone E, then it can be determined that the point tracks are in the F mode. If the frequency jumps to f_3 and the point tracks still appear in zone E, then it can be determined that this is the E mode. By deduction from this principle, the following criterion can be obtained.

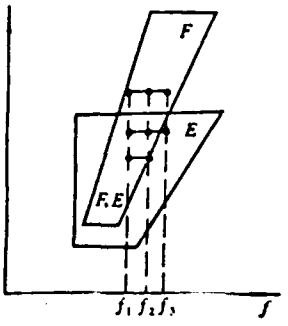

Fig. 1. Schematic diagram of observation zone for P～f ionosphere mode

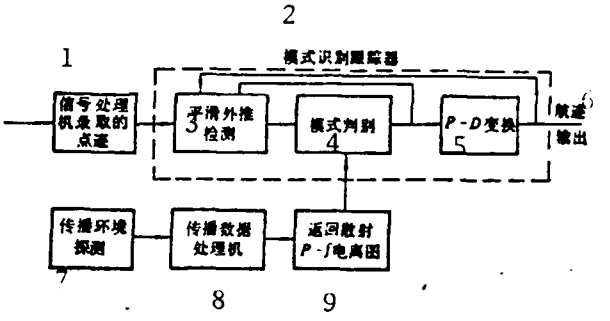

Fig. 2. Pattern recognition tracking device of feedback type
1 - Point tracks recorded by signal processor 2 - Pattern tracker
3 - Smooth extrapolation probe
4 - Pattern determination
5 - P-D transformation
6 - Ground track output
7 - Probe of propagation environment
8 - Propagation data processor
9 - Reentry scattering P-f ionosphere

(1) After necessary observation of the jump frequency, the loci of the target point tracks penetrate to or are included in the not-fuzziness zone mode, then the point track mode is determined by the not-fuzziness zone mode.

(2) In the double fuzziness zone, after the required frequency shift observation, the loci of the target point tracks terminate at the boundary of a mode observation zone, then this is the mode lying within this boundary.

(3) In the triple fuzziness zone, after the required frequency shift observation, if the loci of the point tracks extend to two double-fuzziness zones, then the common mode of these two double-fuzziness zones is the mode of these point tracks. If the loci of the point tracks extend to a double-fuzziness zone, then the mode of the point tracks cannot be determined, remaining still fuzzy. Thereupon, one must suspend or make another frequency jump for the determination.

3. Algorithm of probe tracking

As pointed out by Dewitt's research [2], in OTH-B radar, consideration can be given to two types of filters based on concrete situations; these are the Wiener filter and the Karman filter. In Wiener filtration, an increment in the vector is invariant with time; after computation off-line, this increment in the vector can be used again and again. The increment in the vector determines how fast the tracked coordinates can vary. However, the computational time for the vector increment in a Karman filter is too long, but the computation can derive probability density as useful information for error prediction. If the predicted error is a random variable along with zero mean value asociated with a gaussian distribution, this distribution function can be fed back to the detector along with the predicted value to be used to improve the next frame of the data probe. In

most situations, probe noise is white and has a gaussian distribution; however, mobile noise is colored. Thus, the next-best Karman filter and the expansion type Karman filter changing the colored noise to white can be used. However, in the latter case, computational complexity increases. When there is a diametral direction velocity or constant acceleration of the target is evident, the simplified Karman filter can achieve the optimal outcome. These algorithms can be selected according to the target motion situation.

When a particular type of tracking algorithm is selected, the point tracks of the same mode in a group can be smoothly extrapolated. According to a certain discrimination criterion within the correlated zone of a predetermined wave gate, two gate threshold probes can be executed in order to satisfy the requirements of point tracks in existing the probability P_1 in an observation mode zone to discriminate the propagation mode of the point tracks that are just barely detected. Feedback for smooth extrapolation by using the probe values and the original extrapolated values can be used to obtain the covariance matrix of the estimated positional value; the predicted value and estimated value of the position can be obtained with a particular Karman tracking algorithm. This is a type of feedback mode recognition tracking device, as shown in Fig. 2. Prior to the coordinate transformation, the device first executes pattern recognition and tracking, thus being capable of reducing the execution volume of coordinate transformation of point tracks of these extra modes.

4. Coordinate transformation

Generally, coordinates of OTH-B radar are polar coordinates. The direction of the target is determined by the orientation of the radar wavebeam direction starting from due North. Distance to target is the ground great-circle distance D from the radar

station, but not by multiplying the radar target time delay by the slant distance P of the beam at the speed of light. OTH-B radar is not able to determine target height; however, within the allowable accuracy, only an error less than 20km is introduced. For OTH-B radar, the target height and elevation angle lose significance that they have for ordinary radar. Therefore, the main problem is the P-D transformation, which can proceed point by point with a certain mode corresponding to point tracks. The computation is related to the real-time state of the ionosphere.

For the available P-D transformation methods [3-6], there are the following methods relying on induction: (1) empirical method: this does not consider the real-time change in the ionosphere; the detected P is reduced by a constant (such as 200km); this is the ground great-circle distance D. The error under this method is quite high. (2) Vertical probe stations are set up in the reflected zone of the ionosphere so that the real-time ionospheric parameters or the parameters of the assumed ionosphere mode are derived to solve the beam equation; by using the elevation angle, solve for the P-D relationship. (3) By using the answering unit for calibration as the distance to a reference object, the beam equation can be solved. In the two latter methods, equipment or systems other than radar station should be added. This paper proposes a new algorithm. Its greatest advantage is that the data of point tracks probed with the equipment at a single radar station, and the $P \sim f$ ionization diagram can be used to complete the computations, without having to rely on information data from other probe means outside the radar station.

III. New Algorithm for P-D Transformation

After the author studied the ionosphere reentry probe system in an OTH-B radar station, a $P \sim f$ ionosphere diagram was obtained, thus leading to a new algorithm [7] of ground distance

corresponding to the minimum time delay line in the P∼f diagram. Successively, a new method [8] of the minimum time delay conversion corresponding to random time delay of the divergent fixed target echo in the P∼f diagram is derived. Finally, this method has been extended to the situation [9] when the echo scanning tracks of a moving target in the P∼f diagram are determined. In this paper, these new algorithms are comprehensively applied in the pattern recognition tracking processor of the OTH-B radar in order to determine the tracks of an aircraft target.

1. Conceptual path of algorithm

Fig. 3 is a relationship diagram giving out the experimental data and computational data of the new algorithm for aircraft navigation tracks. As shown in the figure, the minimum time delay line is determined with the ionospheric reentry scattering system. The main radar system provided the point track data of the nontypical fuzziness zone that can be determined only after pattern recognition: time delay P, doppler frequency f_d, working frequency f, and time t. For point tracks P recorded during a probe, the transformation conceptual path of the corresponding ground distance D is to first solve for the minimum time delay P' corresponding to a random time delay P. Then from P', the corresponding ionospheric reflection virtual height h' is derived. Finally, from P' and h' solve for the ground great-circle distance D corresponding to P.

2. Algorithm steps and formulas

(1) For the ionosphere P∼f diagram, preprocessing is conducted on the minimum time delay line and the point track echo scanning track; thus, the K factor array $(k, k_0, k_1, k_2 \ldots)$ of the minimum time delay equation and the point track scanning track equation are derived.

The minimum time delay equation is

$$P'(f)=k_0+k_1f+k_2f^2 \tag{1}$$

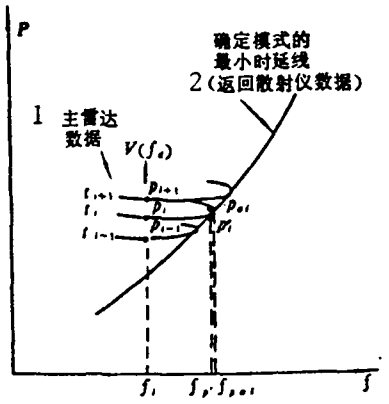

Fig. 3. Relationship between experimental data and computed data
KEY: 1 - Primary radar data 2 - Minimum time delay line for determining the pattern (data of reentry scattering instrument)

When approaching the minimum time delay line, the target point track echo scanning track equation is

$$(f-f_0)=k(P-P_0)^2 \tag{2}$$

In the equation, P_0 and f_0 are coordinates of the vertex of the parabolic scanning track. The various k factors can be derived by using regression as a technique on the data from the ionosphere $P \sim f$ diagram.

(2) With the target point track data f, P, f_d, and t as well as the various k factors of the three radar sets of time series, by using

$$V=-cf_d/2f \tag{3}$$

and

$$(f_i-(S_i-k_0+Vt_{i-1})/k_1)(P_{i+1}-S_i-Vt_i)^2=(f_{i+1}-(S_i-k_0+Vt_i)/k_1)(P_i-S_i-Vt_{i-1})^2 \quad (4)$$

solve for the equivalent distance factor S_i. In the equations, i - 1, i, and i + 1 are quantities corresponding to the instance t_{i-1}, t_i, and t_{i+1}.

(3) From S_i, t_{i-1}, and V, as well as the various k factors, by using the target point parabolic scanning track equation and the vertex coordinate formula

$$P_{0i}=S_i+Vt_{i-1} \quad (5)$$

and

$$f_{0i}=(S_i-k_0+Vt_{i-1})/k_1 \quad (6)$$

solve for the parabolic vertex P_0 and f_0.

(4) From the vertex coordinates and the various k factors, by using the formulas

$$P'_i=P_{0i}+1/(2kk_1) \quad (7)$$

and

$$f_{p'_i}=(P'_i-k_0)/k_1 \quad (8)$$

solve for the minimum time delay coordinate P' and f_p. of the target point tracks.

(5) From the minimum time delay P'_i and $f_{p'_i}$, by using the formula

$$(r_0+h'_i)^2-r_0^2=\frac{P'_i}{2}\left[\frac{k_1P'_i}{\left(k_1+\frac{ak_1P'_i}{1+a(P'_i-2h'_i)}-\frac{P'_i}{f_{p'_i}}\right)}-\frac{P'_i}{2}\right] \quad (9)$$

(In the equation, a = 4.7 x 10^{-5}/km, r_0 = 6370km as the earth's radius), solve for the ionospheric reflection virtual height h' at that instant.

(6) From P'_i and h', by using the formula

$$D_i=2r_0\cos^{-1}[(r_0^2+r_i^2-P'^2_i/4)/2r_0r_i] \quad (10)$$

(In the equation $r_i = r_0 + h'_i$), solve for the ground great-circle distance D corresponding to P.

Compute steps (2) - (6) as a flow cycle, conduct the P-D transformation point by point in the nontypical fuzziness zone, then the diametral-direction ground distance of the target along the direction can be determined from the wavebeam orientation. Details of the derivations for the above-mentioned computation formulas (Eqs. (1) through (10)) are shown in the references [7-9].

IV. Processing Results of the Experimental Data

Used in verifying the algorithms in the paper for its feasibility, the experimental data were provided by an experimental OTH-B radar system; the detection energy of this radar system is 97dB·joule. The firing array is an eight-unit vertically polarized logarithmic cycle antenna fan array; the reception array is a thirty-two-unit vertically polarized logarithmic cyclic antenna straight-line side-firing array with a diameter of 300m. The radars employ a linear modulating frequency pulse doppler system. In the general situation, the working parameters of the radar are as follows: 90kW as the average power, 3.5ms as the pulse duration, 150Hz as the pulse repetition rate, and 5s as the coherent cumulative time. As provided by the radars, the data covered different seasons over a three-year span. There were probe data for a total of 40 batch times of various aircraft models, including large B747 aircraft and small Jian6 fighters.

By using the above-mentioned methods, the probe target point track data of the radar are reprocessed; a comparison is made between the computed results and the ground track data reported by the ground navigation station. The computed results are in agreement with the test results. The mean deviation between the

computed tracks and the actual tracks is less than 4 percent. Fig. 4 gives an example of processing results of two tracks. Fig. 4a shows the tracks of a B707 aircraft, flight number PK752, observed on 19 December 1982. Three frequencies of 20.5, 18.5, and 14.5MHz were used in the track probe. Fig. 4b shows the tracks of a B707 aircraft, flight number CA948, observed on 22 December 1982. Two frequencies of 22.0 and 14.5MHz were used in the track probe. In the figure, a "+" shows the location of the navigation station along the air route. A "·" and a "o" are point tracks of the target ground great-circle distance employed in computations. In the former case, these are point tracks of 1F pattern transmission; in the latter case, these are the point tracks of pattern transmission for layer E_i. The results in the figure show the match between the radar computational results and the actual navigation tracks.

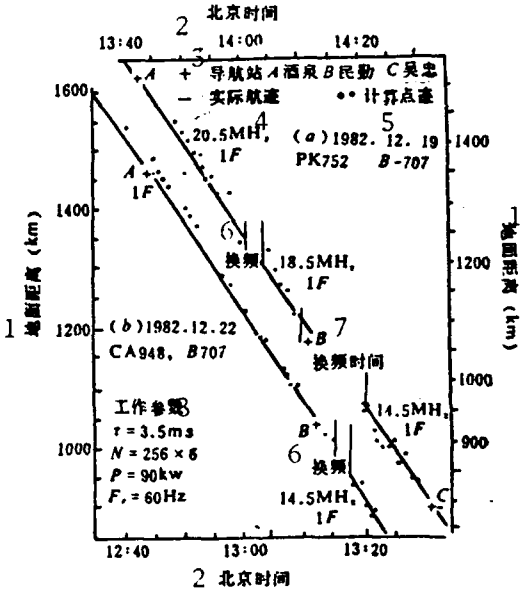

Fig. 4. Two examples of processing results on navigation tracks
KEY: 1 - Ground distance 2 - Beijing time
3 - Navigation station 4 - Actual navigation tracks 5 - Computed navigation tracks
6 - Frequency shift 7 - Time of frequency shift
A - Jiuquan B - Minqin C - Wuzhong

V. Conclusions

In the paper, the pattern recognition, tracking, and data processing method for coordinate transformation for the navigation track processing of OTH-B radar are given; a new algorithm for coordinate (P-D) transformation is proposed. In the algorithm, it is not required to assume the data or to rely on the data of ionospheric probe means outside the radar station; the only data used are from the probe relying on equipment at a single OTH-B radar station. The algorithm has unique features of fewer processing data, high real-time property status and computational simplicity.

By using this method for processing the target point track data observed by an experimental OTH-B radar system, the mean deviation between the observed data and the actual navigation tracks is less than 4 percent. The results verify the feasibility and application accuracy of this method.

The experimental data in the paper were provided by the Nanjiang Research Institute of Electronics Technology, and the Over-the-Horizon Radar Experimental Team of the China Research Institute of Radio Wave Propagation. Bao Yanghao and Du Junhu furnished valuable comments on the paper. The author expresses his gratitude to those mentioned above.

The first draft of the paper was received in June 1989; the final draft was received in February 1990.

REFERENCES

1. Headrick, J. M. and Skolnik, M. I., PIEEE 62/6, 664-671 (1974).
2. Dewitt, P. N., AD-A013648.

3. Li Chonggeng, Xiandai Leida [Modern Radar] 6/4-5, 276 (1984).
4. Chernov, Yu. A., Vozvratno-nakloniye Zondirovaniye Ionosfera [Slant-Return Ionosphere Probes], 1971.
5. Croft, T. A., Radio Sci., No. 3, 69-74 (1968).
6. Huang Xiwen and Li Yongjun, Dianbo Koxue Xuebao [Radio Wave Science] 1/2, 36-42 (1986).
7. Jiao Peinan and Zhu Qiguang, Wuhan Daxue Xuebao [Journal of Wuhan University] 4, 63-70 (1985).
8. Jiao Peinan and Du Junhu, Kongjian Koxue Xuebao [Space Science] 7/1, 59-64 (1987).
9. Du Junhu and Jiao Peinan, Kongjian Koxue Xuebao 7/3, 229-233 (1987).

DISTRIBUTION LIST

DISTRIBUTION DIRECT TO RECIPIENT

ORGANIZATION	MICROFICHE
B085 DIA/RTS-2FI	1
C509 BALLOC509 BALLISTIC RES LAB	1
C510 R&T LABS/AVEADCOM	1
C513 ARRADCOM	1
C535 AVRADCOM/TSARCOM	1
C539 TRASANA	1
Q592 FSTC	4
Q619 MSIC REDSTONE	1
Q008 NTIC	1
Q043 AFMIC-IS	1
E051 HQ USAF/INET	1
E404 AEDC/DOF	1
E408 AFWL	1
E410 ASDIC/IN	1
E411 ASD/FTD/TTIA	1
E429 SD/IND	1
P005 DOE/ISA/DDI	1
P050 CIA/OCR/ADD/SD	2
1051 AFIT/LDE	1
P090 NSA/CDB	1
2206 FSL	1

Microfiche Nbr: FTD93C000497
FTD-ID(RS)T-0853-92